International Journal of Engineering Inventions
e-ISSN: 2278-7461, p-ISSN: 2319-6491
Volume 11, Issue 10 [October. 2022] PP: 143-152

Investigation the Thermo-Hydraulic Performance for Solar Air Heater Roughened With Semicircular Baffles Numerically

Ahmed F. Khudheyer
Al-Nahrain University, engineering college, Baghdad, Iraq.

Asim M. Abdul Wahab
Al-Nahrain University, engineering college, Baghdad, Iraq.

Abstract

The numerical study of turbulent streams through such a solar air heating element leathery texture with semicircular partitioned transversal ribs imperfection was carried out. A set of governing equations represents the physical issue theoretically, and the transportation equations can be solved by using numerical simulation technique. According to the numerical conclusions, the flow-field, typical Nusselt number, and mean friction factor are all substantially dependent on the relative roughness height. For a comparative coming up of 0.042, the thermal and hydraulic overall performance is discovered as being the highest. Comparisons between previously published research were made, and reasonable fit is discovered.

Keywords: CFD, SAH, roughened, semicircular, thermo, hydraulic, performance

---

Date of Submission: 14-10-2022 Date of Acceptance: 30-10-2022

---

1. Introduction

One kind of heat exchanger known as a solar air heater works by converting the thermal energy produced by solar radiation into usable heat. Conventional solar air heaters have a low thermal efficiency largely because of significant heat losses and a low convective heat transfer coefficient between the absorber plate and the flowing air stream. This results in a higher absorber plate temperature and larger thermal losses. The air flow duct is generated when the absorber and the bottom plate come together to form a channel. Within this channel, the air is heated by the solar radiation that is absorbed by the absorber [1, 2]. Methods that enhance the large heat transfer region, such as claws or corrugated coatings [3-5] and layer thickness [6-8], and methods that significantly raise turbulence well within broadcaster, such as these, include the most popular and effective ways to increase the rate of convective heat transfer in channel flows.There are many other effective strategies, but these are the most common and successful ones. It is a well-established fact that the application of artificial roughness in a variety of various forms and shapes is the most efficient and cost-effective method for enhancing the efficiency of a solar air heater. One of the passive strategies that is used most often for the purpose of improving heat transmission is the application of artificial roughness to a heated surface. The increase in heat transfer will always be accompanied by a corresponding increase in the pressure drop that is incurred by the fluid flow.

Tiny wires of varying sizes, forms, and rotations on the underside of the base plate are a distinguishing characteristic of intentionally rough surface solar-powered air heaters. It has been proposed that major and efficient design modifications may boost efficiency of heat transfer. In attempt to increase the heat transfer coefficient also with minimal possible of pumping capacity, several experimental attempts have been undertaken to improve the thermal efficiency of conventional solar air heaters by using roughness elements of varying shapes, dimensions, and alignments.The laminar sub-layer, which is located extremely near to the duct surface, is the only place where turbulence may be produced in order to maintain minimal friction losses. Only a short overview of the artificially roughened solar air heater is provided here. Readers are directed to references [9–11] for further information in detail.

The term "computational fluid dynamics" (CFD) refers to a numerical flow modeling tool that enables virtual flow testing capabilities and provides in-depth insight into flow and thermal fields for the purpose of improving design analysis and making enhancements. Numerical techniques are used to solve the governing equations, which include the conservation of mass, momentum, and energy, in order to do an analysis of the fluid flow issues. For the purpose of simulating the interaction of fluids (gases and/or liquids), with object surfaces that are defined by appropriate boundary and starting conditions, computational power is employed to complete the calculations that are necessary to do so. The use of high-performance computing allows for the development of solutions that are both faster and more effective. As an alternative to time-consuming and financially burdensome testing of expensive real-world physical prototypes, computational fluid dynamics (CFD) enables comprehensive simulation of multi-physics capabilities, allowing for early classifiers in the product development process. This gives them a significant edge over their competitors since they are able to get a more robust and efficient design to market faster and with less overall cost.Over the course of the last ten years, CFD has found use in a wide variety of engineering subfields; as a result of our tremendous excitement, we are delighted to explore new boundaries in a variety of companies. Because of advancements in both processing power and CFD tools, it is now feasible to do an analysis of the flow structure that is far more detailed than was previously conceivable.

It has been observed, on the basis of an overview of the previous work in the field of artificially rough surfaces thermal performance, that very few initiatives have been taken to model and simulate an artificially roughened solar air heater. This observation is based on the fact that there have been very few attempts made.Yadav and Bhagoria [12] made a mathematical simulation to analyze solely the thermal performance behaviour of a rectangular channel of a solar-powered air heater that had triangular rib roughness upon that absorber plate. Their focus was on the conduct of heat transfer. The relative roughness pitch of 10 was discovered to correlate to the Nusselt number's highest value, which was determined to be 10. Using computational fluid dynamics (CFD), Chaube et al. [13] analyzed the temperature distribution and fluids flow properties of a synthetically roughened solar-powered air heater having ten distinct ribs forms, including circular, hemispheric, rectangular, predrilled, triangular, etc.This analysis was conducted on an artificially roughened solar air heater with 10 different ribs shapes provided on the absorber plate. The scientists observed that, out of the 10 various kinds of rib shapes that were employed, the one that provided the highest performance was a rectangular rib. Yadav and Bhagoria [14] used computational fluid dynamics to report their analysis of Artificial coarse texture solar heating element with such a circular crosswise cable rib imperfection on the base plate for improved temperature transfer and fluid flow (CFD). Using the ANSYS FLUENT 12.1 code, a two-dimensional computational fluid dynamics (CFD) simulation was carried out. It was determined that the Renormalization Group (RNG) k-e model would be the best applicable choice. For the spectrum of parameters that were looked at, the highest possible value of the thermal enhancement factor was discovered to be 1.65. A computational fluid dynamics (CFD) examination of the fluid flow and heat transfer properties of a solar air heater with arc-shaped rib roughness on the absorber plate was carried out by Kumar and Saini [15]. For the purpose of simulating the fluid flow and heat transmission, the Renormalization group (RNG) k-e model was used.
Artificial coarse texture solar heating element with such a circular crosswise cable rib imperfection on the base plate for improved temperature transfer and fluid flow (CFD). A commercial finite volume program the characteristics of the flow of air via the duct of a standard solar air heater were analyzed with the help of ANSYS FLUENT 12.1. It was discovered that the Nusselt number rose as the Reynolds number rose, whereas the friction factor fell as the Reynolds number rose. This was the opposite of what was found to be true for the friction factor. Karmare and Tikekar [17] conducted a computational fluid dynamics assessment of fluid flow and heat transfer in a solar air heater duct that had metal grit ribs as the roughness components. As a problem solution, the commercial CFD code FLUENT 6.2.16 was used. For the purpose of simulating turbulent airflow via an artificially roughened solar air heater, a Standard k-e turbulence model was used. According to the scientists' findings, the absorber plate that had a square cross-section rib and a 58 angle of attack offered the greatest results out of all of the alternative forms and orientations that were investigated. After considering the irregularity of the bottom of the upper heated wall as rectangular shape transverse ribs, Yadav and Bhagoria [18] undertook a numerical study of the heat transmission and flow friction properties in an intentionally rough surfaces solar air heater. This roughness was considered at the artificially roughened solar air heater's top heated wall. In order to investigate the relative roughness pitch's impact on the system as a whole, a calculation was made to determine the thermohydraulic performance parameter while adhering to the same pumping power restriction. It was discovered that the thermohydraulic performance parameter may reach its maximum value of 1.82, which corresponded to a relative roughness pitch of 10.71. A numerical study was conducted out by Gandhi and Singh [19] to examine the impact of artificial surface quality on stream through a corrugated channel that had a bottom surface that has been abraded with parroted transverse ridges of an abutment transformed cross-section. The bottom facade of the tube was coarse texture with a funnel pass.This was done in order to investigate the effect that the artificial surface roughness had on the flow. A comparison was made

between the numerical findings generated by the commercial computational fluid dynamics (CFD) code FLUENT and the experimental data. The scientists also noticed that the outcomes of the CFD simulations were in excellent agreement with the experimental findings that were readily accessible. Yadav and Bhagoria [20] is the reference that readers should go to for additional information regarding the many CFD experiments that were conducted on roughness components of varying forms, sizes, and orientations.An exhaustive review of the relevant literature reveals, among other things, that very little CFD investigation has been carried out on an artificially roughened solar air heater with semicircular sectioned transverse rib roughness on the absorber plate. This is one of the findings that emerges from the review.
The goal of this project is to do such an investigation using the cfd Simulation program ANSYS FLUENT 2022R2.Herein, we use a computational fluid dynamics (CFD) method to compare the thermal - hydraulic performance of a solar-powered heat transfer using and without an artificially roughened absorber plate.This study employs artificial roughness in the form of a crosswise rib with a semicircular cross section to improve heat conduction. The primary objective of this work is to utilize a computational fluid dynamics (CFD) approach to examine the impact of relative roughness height on average Nusselt number, average friction factor, and thermohydraulic results displayed in a synthetically rough surfaces solar air heater with semicircular sectioned circumferential rib coarseness.
In this study, we utilize the computational fluid dynamics (CFD) code ANSYS FLUENT 2022R2 and its companion programs, ANSYS DESIGN MODELER 2022R2 and ANSYS ICeMCFD 2022R2, to simulate the heat flow and friction factors of a solar air heaters that has been artificially abraded.

Processes of Modelling and Simulating

By using finite-volume approach to solving the mathematical model, the CFD application software ANSYS FLUENT is used to perform a 2-dimensional CFD model of a solar air heater that has been purposely roughened. In the parts that follow, it'll go through the computing domain and the numerical method.Computer SimulationANSYS DESIGN MODELER was used to develop a computational model.

In Fig. 1, a rectangle stands in for the finite element model of a solar-powered air heater that has been intentionally coarse texture. The use of a significantly difficult and costly three - dimensional model could be managed to avoid by using an appropriate 2-D computational model simulates the turbulent flow and forced-convection features of an artificially rough surfaces solar air heater with a radial rib on the absorber surface, as proposed by Yadav and Bhagoria [14]. The 2-D computational domain was selected for this study due to the space and time savings it would provide. The domain had three levels: the starting level (L_1), the testing level (L_2), and the final level (L_3). For a roughened duct, the thermally completely developed flow is created in a short length of just a couple of times the hydraulic diameter, therefore a short entry length is selected in accordance with ASHRAE Standard [21]. In order to lessen the impact of the exam itself, the departure section is employed following it. The duct's interior cross section is 100 mm* 20 mm.

The relative roughness pitch (P/e =14.29) has been held constant over three iterations of rib-pitch (P) and rib-height (e). The Reynolds number, Re, ranges from 3800 to 18,000 (important in a solar air heater), while the relative roughness height, e/D, ranges from 0.021 to 0.06. Thermohydraulic considerations led Gupta et al. [22] to conclude that solar air heater systems operating within a narrow Reynolds number range (3800-18,000) would exhibit superior thermohydraulic performance.

An aluminum solar collector 0.5 mm in thickness makes up the upper panel.The absorber plate is assumed to be plain on all sides except for the bottom of a head of a conduit, which is assumed to have an artificial roughness in the shape of a semicircular sectioned transverse rib. To ensure that the laminar sub-layer is on the same order as the roughness height and that fin=flow passage obstruction effects may be insignificant, the minimum and maximum square rib heights have been set to 0.7 and 2 mm, respectively. In the numerical study, the top of the absorber plate is assumed to be subjected to a homogenous heat flux of 1000 W/m^2.
Table 1 details the geometrical and operational parameters used in this CFD study. Figure 2 depicts a typical roughened absorber plate with a variety of semicircular sectioned transverse rib roughness configurations.

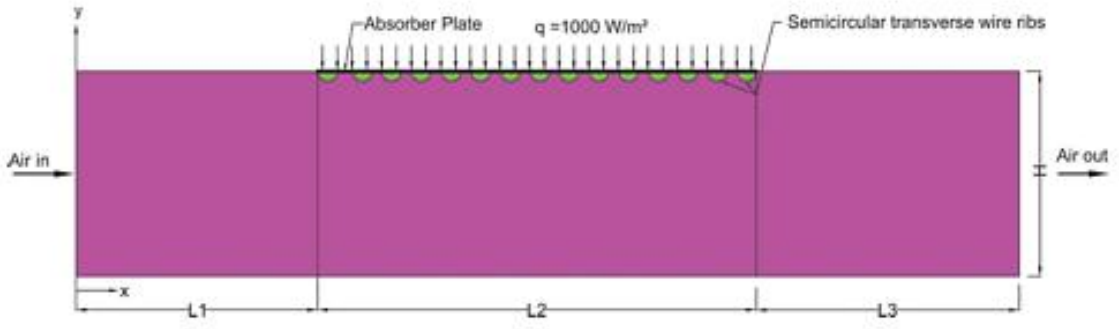

Fig.1 computational domain

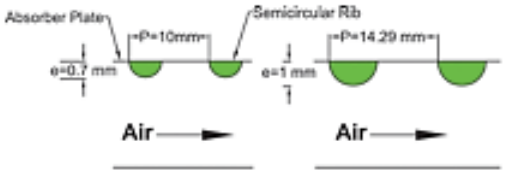

Fig. 2 roughened absorber plate schematic

Table 1. Range of geometrical and operating parameters for CFD analysis

Geometrical and operating parameters	Range
Entrance length of duct, L_1	245 mm
Test length of duct, L_2	280 mm
Exit length of duct, L_3	115 mm
Width of duct, W	100 mm
Depth of duct, H	20 mm
Hydraulic diameter of duct, D	33.33 mm
Duct aspect ratio, W/H	5
Rib height, e	0.7, 1.0,1.4 and 2 mm
Rib Pitch, P	10, 14.29,20 and 28.58 mm
Reynolds number, Re	3800–18000 (6 values)
Prandtl number, Pr	0.7441
Relative roughness pitch, P/e	14.29 (fixed value)
Relative roughness height, e/D	0.021, 0.03,0.042 and 0.06

Grid Distribution

In just this study, non-uniform meshes were produced for use in all of the computational models that are carried out. In simulation, quasi matrices are frequently used where it is anticipated that substantial gradients will be present, when local features are sought, or when complicated geometries are found. All of the numerical simulations that were carried out for this study used non-uniform grids that were automatically produced (and conformed to patches). The program ANSYS ICEM CFD 2022R2 is used to produce the grids. For the purpose of resolving the laminar sublayer, a non-uniform grid comprising 411238 quad cells and having a cell size of 0.2 mm was used, as seen in Fig. 3. After increasing the mesh density and using a variety of mesh grading, a series of exhaustive tests are performed in order to validate the grid independence of the model. These tests continue until additional refinement reveals a difference of less than one percent between two sets of findings.

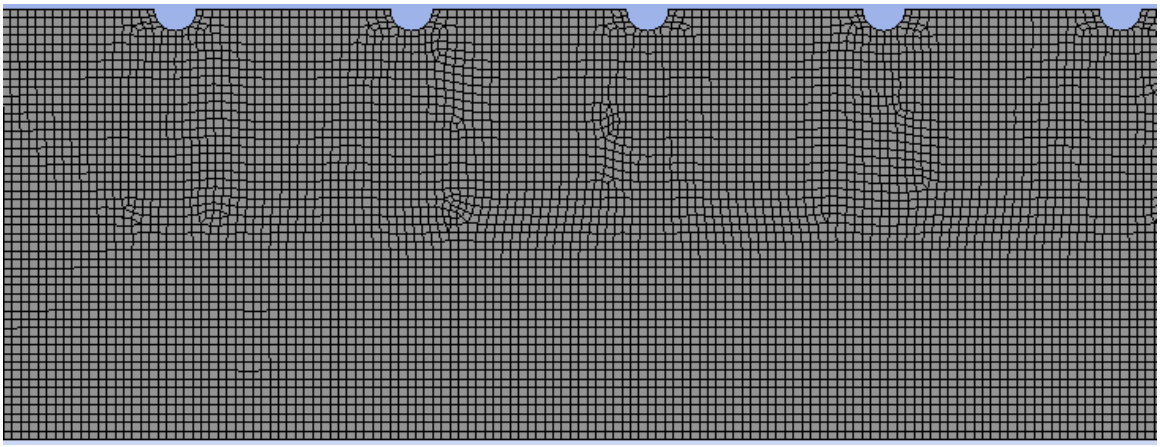

Fig. 3 meshing for the computational domain

Governing Equation

The computational fluid dynamics (CFD) approaches include the approximate results of problems involving the preservation of mass, momentum, and energy, together with additional equations such as those involving species movement. The equations in question may be solved by using various numerical algorithms and techniques. The following is a summary of the governing equations in a two-dimensional space.

Continuity equation:

$$\frac{\partial}{\partial x_i}(\rho u_i) = 0 \qquad 1$$

Momentum equation:

$$\frac{\partial}{\partial x_i}\left(\rho u_i u_j\right) = -\frac{\partial p}{\partial x_i} + \frac{\partial p}{\partial x_j}\left[\mu\left(\frac{\partial u_i}{\partial x_j} + \frac{\partial u_j}{\partial x_i}\right)\right] + \frac{\partial}{\partial x_j}\left(-\rho\overline{u_i'u_j'}\right) \qquad 2$$

Energy equation:

$$\frac{\partial}{\partial x_i}(\rho u_i T) = \frac{\partial}{\partial x_j}\left((\Gamma + \Gamma_t)\frac{\partial T}{\partial x_j}\right) \qquad 3$$

$$\Gamma = \mu/\mathrm{Pr} \text{ and } \Gamma_t = \mu_t/\mathrm{Pr}_t$$

Boundary conditions

A homogenous air flow is provided at the input of the solar air heater that has been artificially roughened, and an outlet pressure exit state with a fixed pressure of 1.013*105Pa is applied at the exit. It is considered that the air's 300 K continuous velocity with in direction of flow.The air within the duct is likewise assumed to be 300 K atstarting point. It has been pre-summited that the air's physical characteristics would never change.At the bulk average temperature the conducting fluid's thermo - physical properties characteristics, as well asTable 2 includes a list of absorber plates. Criteria for an impermeable border and a non-slip wallbeen put into place above the ducting walls.There at absorber surface (upper panel), a continuous influx of 1000 W/m ^{2} is applied, with the bottom surface maintained in an isothermal state.

Turbulence model

Because it produces results that are more similar to those produced by the Dittus–Boelter empirical correlation and the Blasius empirical correlation, the Mathematical formalism (RNG) k-e model was chosen to be used in the existing computer model to visualize the thermal performance and transport phenomena characteristic. This decision was based on the outcomes produced by the model being closer to those produced by the Blasius empirical correlation. A comprehensive description of how to choose the most appropriate transport equations for the modeling of an intentionally roughened solar air heater can be found in another study authored by the same authors [20]. It may go here for more information on an alternative turbulence.

$$\frac{\partial}{\partial x_i}(\rho k u_i) = \frac{\partial}{\partial x_j}\left(\alpha_k \mu_{eff}\frac{\partial k}{\partial x_j}\right) + G_k - \rho\epsilon \qquad 4$$

$$\frac{\partial}{\partial x_i}(\rho c u_i) = \frac{\partial}{\partial x_j}\left(\alpha_\varepsilon \mu_{eff}\frac{\partial \varepsilon}{\partial x_j}\right) + \mathrm{C}_{1\varepsilon}\frac{\varepsilon}{k}(G_k) - \mathrm{C}_{2\varepsilon}\rho\frac{\epsilon^2}{k} - R_E \qquad 5$$

$$G_k = -\frac{\rho \overline{u_i' u_j'} \partial u_j}{\partial x_i} \quad 6$$

$$\mu_{eff} = \mu + \mu_t \quad 7$$

$$\mu_t = \rho C_\mu \frac{k^2}{\varepsilon} \quad 8$$

CFD solution

After all of the mathematical model have been designed and simulated to use an upwind-biased method of the second order and a finite volume technique, the variables have been solved in a compartmentalized way.
In order to formulate the equations, a professional item of computational fluid dynamics (CFD) application system ANSYS FLUENT 2022R2 is utilized. For the calculation of incompressible viscous, using semi-implicit technique for pneumatically expressions (SIMPLE) approach to connect both pressure and velocity has been used [25]. In this particular computational fluid dynamics (CFD) inquiry, the Renormalization-group (RNG) k-e model has been used to simulate both the flow and the thermal expansion. The value 0.001 has been chosen as that of the convergence criterion for each and every dependent variable. Whenever converging issues are found, the approach is begun using the first order upwind considering the target and then proceeded with the 2nd order upwind technique. This process is repeated till the issue is resolved. At the same time as a consistent air flow is being provided at the input, a pressure (fixed) outlet state is being maintained at the exit. Although a steady heat flux criterion has indeed been provided to the top duct wall of the test rig, a thermal parameter has really been established over the bottom duct wall.

2. Results and Discussion

CFD calculations of heat transmission and fluid flow properties in an artificially rough surfaces solar air heater with such a longitudinal rib with such a semicircular cross-section. The following section will examine the impact of mesh concentration, Reynolds number, and roughly comparable trying to reach (e/D) on the mean frictional and heat transfer qualities for flow of air inside an arbitrarily roughened solar heater. These characteristics include average thermal performance and turbulence

Mesh independence

An implementation of something like a grid independence check is carried out over arrays that include varying amounts of cells; specifically, 221,638, 342,184, 411,238, and 498,125 are employed throughout the four stages. When increasing the number of cells between 411,238 to 498,125, it was discovered that the variance in Skin friction coefficient increased by only a little amount. Because of this, expanding the number of cells beyond this figure will not result in any advantageous outcomes. As a result, the grid structure consisting of 411,238 cells has been selected for this particular calculation.

Heat transfer characteristics

Figure 4 shows how the roughly comparable irregularity height (e/D) affects the mean Nusselt number. A plot of the average Nusselt value vs Reynolds number is shown in Figure 4 over a range of relative roughness heights (e/D) and a constant relative roughness pitch (P=e) of 14.29. As predicted, a rise in Reynolds number leads to an increase in the average Nusselt number. The roughness components become more noticeable with higher Reynolds numbers.further than sublayer. Reynolds number reduces laminar sublayer height. Roughness-generated vortices also contribute locally to energy dissipation. Relative to a flat surface, this boosts heat transmission. Nusselt number grows with relative roughness height (e=D) for given relative roughness pattern (P=e). Greater overall roughness height creates strong fluid motion by reattaching free shear layer. Heat transmission rises with roughness height and peaks at e=D=0.06.
Also it depicts the fluctuation of Nusselt number ratio (enhancement ratio) as a consequence of Reynolds number with varied proportional roughness height (e=D) and pitched (P=e) quantities of 14.29. With increasing Reynolds number, when Nusselt number proportion climbs, reaches a maximum, and then drops. The highest increase in Nusselt number was 2.34 times for a plain tube at a Reynolds number of 15,000.Increased Reynolds figure grows turbulence kinetic or dissipation ratio, which raises pressure distribution with Nusselt number.

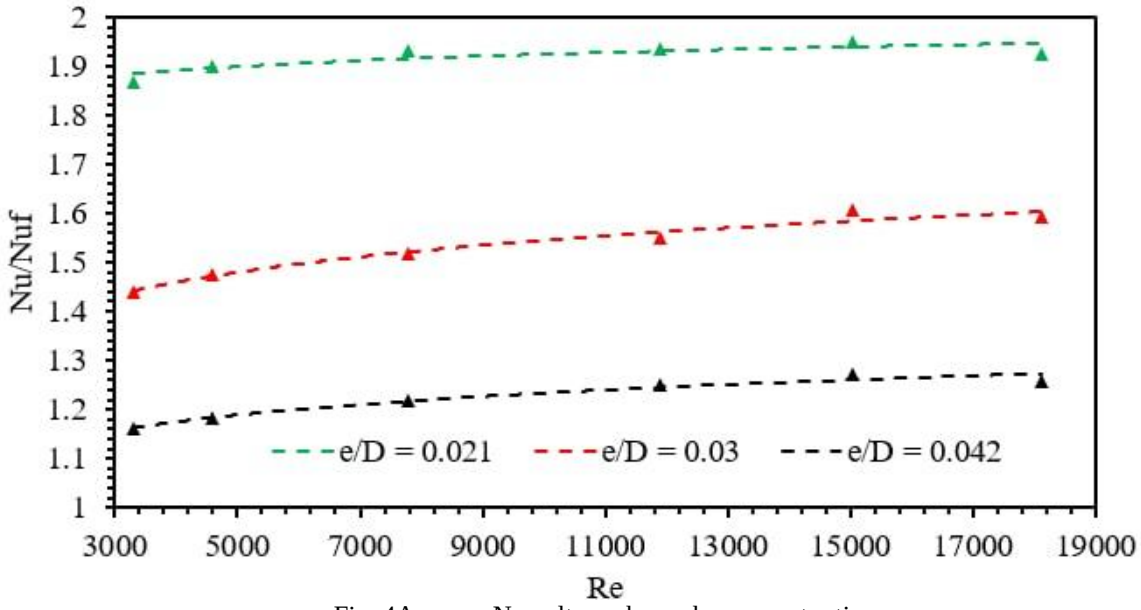

Fig. 4Average Nusselt number enhancement ratio

Friction factor

The cartogram of kinetic energy from turbulence helps us make sense of heat transport events. Figure 6 is a contours plot of both the angular momentum of turbulence over a range of comparative roughness height (e/D) with Reynolds number (12,000) and relative roughness pitches (P/e) levels (14.29). The nearest heated wall upon that downstream face of such rib is where the angular momentum of turbulence was highest; farther further away from the wall, the kinetic energy of instability drops down. The contour map of entropy generation may also be used to evaluate and characterize other heat transport events.

Figure 6 is a contour plot of entropy generation vs relative roughness height (e/D) once at constant Reynolds number (12,000) and relative roughness pitch (P/e) of 14.29. As one moves away from the upstream side of the rib, the turbulence strength reduces until it reaches a minimum far downstream of the top heated wall. Roughness elements become visible outside of the laminar sub-layer as the Reynolds number grows; the thickness of the laminar sub-layer thins as the Reynolds number rises. In addition, the roughness itself contributes locally to the heat removal via the vortices. At a constant Reynolds number of 12,000 and relative roughness pitch (P/e) of 14.29, the heat transfer rate is improved relative to a smooth pressure surface of varying e/D values. As predicted, a smaller pressure drop results in a smaller relative roughness height, while a larger pressure drop results in a larger relative roughness height.

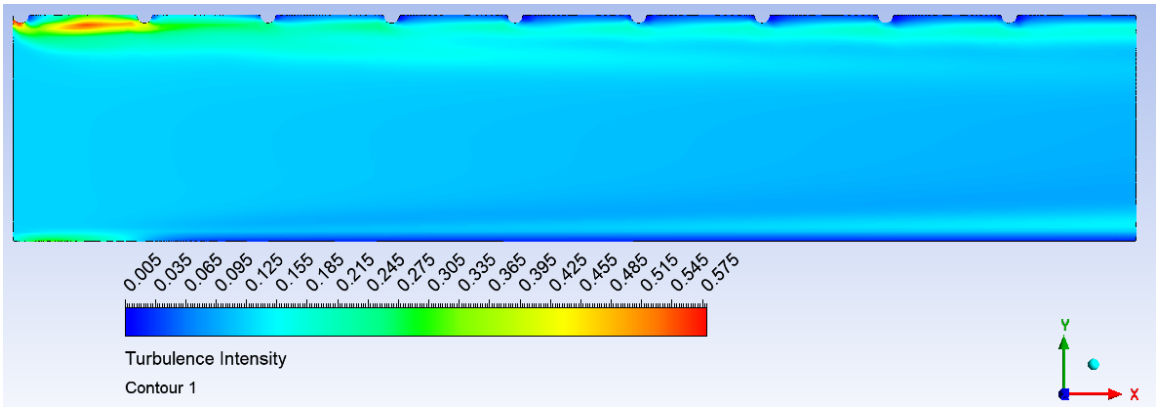

a

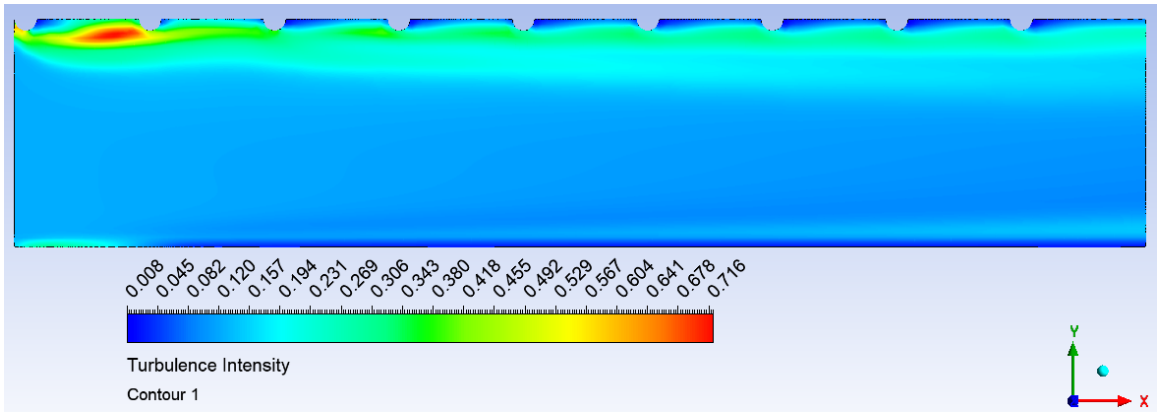

b

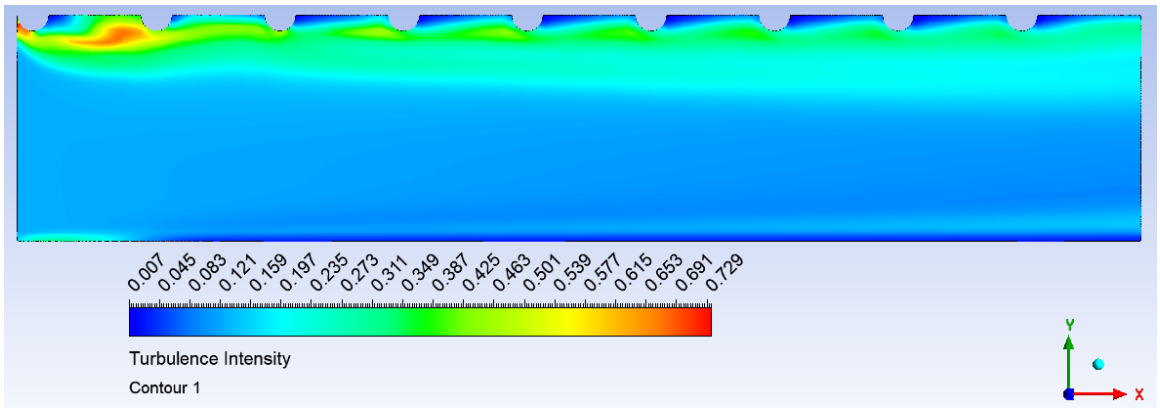

C

Figure 6. Contour plot of turbulent kinetic energy for Re = 12000 and P/e = 14.29 at a relative roughness height of (a) e/D = 0.03, (b) e/D = 0.042, and (c) e/D = 0.06

Thermo-hydraulic performance

Figure 7 depicts how well the thermo hydraulic system performance varies with both the Reynolds number for just a variety of relative roughness tallness (e/D) virtues and a constant relative roughness infield (P/e) valuation of 14.29. Additionally, this variation is shown for a single relative roughness pitch (P/e) value. It is plain to observe that now the thermal properties performance parameters are almost always greater than one for every conceivable scenario. With an increasing Reynolds number, the thermo hydraulic performance parameter has a tendency to grow at first, then decline after a while. For the spectrum of characteristics that were looked at, it was discovered that the results for the thermal and hydraulic control factors ranged anywhere from 1.17 to 1.71.

Once at Reynolds number of 15,000, it was discovered that a solar air heater that had been roughened with semicircular sectioned transverse rib roughness on the absorber plate provided the better thermo hydraulic performance parameter. As a result, this solar air heater could be used for heat transfer enhancement.

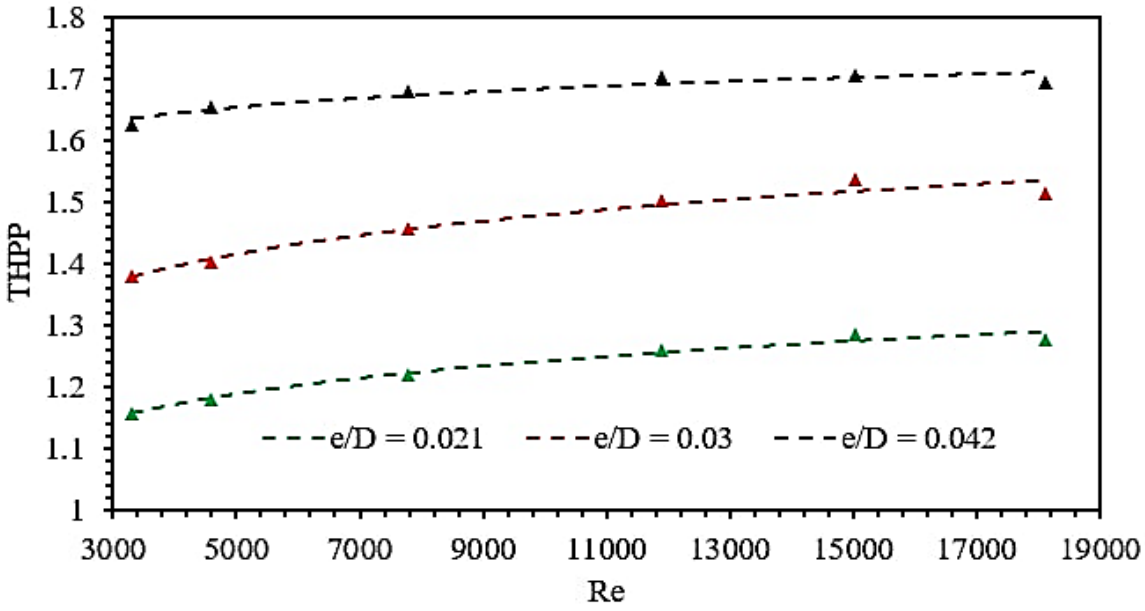

Fig. 7 effect of relative roughness height on thermal hydraulic performance parameter

3. Conclusions

The two-dimensional computational model is built in order to forecast the effectiveness of a solar air heater that includes an absorber plate that is roughened using semicircular sectioned transverse rib roughness. This model was constructed using a semicircular partitioned transverse rib harshness. According to the numerical findings, the flow field, the average Nusselt number, and the mean friction coefficient are all highly reliant just on roughness pitch. In light of the current forecasts provided by CFD, the following set of pertinent conclusions may be derived.

1. Roughness altitude and pitch impact flow direction as well as solar air heater efficacy. The absorbent plate's semicircular crosswise rib irregularity improves heat transmission.
2. Highest Nusselt number percentage is 2.34, equal to 0.06 roughly comparable roughness height at a Reynolds number of 15,000.
3. Greatest skin friction coefficient ratio is 1.92, equal to relative roughness height of 0.06 at Reynolds number 3,800.
4. Improved thermo hydraulic performances is achieved by creating turbulences solely in the laminar sub-layer area of the shear layer.
5. At such a Reynolds number equal 15,000, it is discovered that now the solar air heater coarse texture with semicircular partitioned transverse rib roughness on the absorber plate with e/D =140.042 gives the superior thermo hydraulic performance parameter.
6.

NOMENCLATURE

C_p	specific heat of air, J/kg k
D	equivalent or hydraulic diameter of duct, mm
e	rib height, mm
e/D	relative roughness height
f	friction factor
H	depth of duct, mm
h	heat transfer coefficient, W/m^{2}K
k	thermal conductivity of air, W/mK
L	length of duct, mm
L_1	inlet length of duct, mm
L_2	test length of duct, mm
L_3	outlet length of duct, mm
Nu	Nusselt number
P	pitch, mm
P/e	relative roughness pitch
Pr	Prandtl number
Re	Reynolds number
v	velocity of air in the duct, m/s
W	width of duct, mm
W/H	duct aspect ratio
α	angle of attack, degree
Γ	molecular thermal diffusivity, m^2/s
Γ_t	turbulent thermal diffusivity, m^2/s
δ	transition sub-layer thickness, mm
ΔP	pressure drop, Pa
ε	dissipation rate, m^2/s^3
κ	turbulence kinetic energy, m^2/s^2
μ	dynamic viscosity, Ns/m^2
μ_t	turbulent viscosity, Ns/m^2
ρ	density of air, kg/m^3
ω	specific dissipation rate, 1/sec

Subscripts

r	roughened
s	smooth

References

[1]. J. A. Duffie and W. A. Beckman, Solar Engineering of Thermal Processes, Wiley, New York, 1980.
[2]. A. S. Yadav and J. L. Bhagoria, Renewable Energy Sources—An Application Guide, Int.J. of Energy Sci., vol. 3, no. 2, pp. 70–90, 2013.
[3]. D. M. Ferley and S. J. Ormiston, Numerical Analysis of Laminar Forced Convection in Corrugated-Plate Channels with Sinusoidal, Ellipse, and Rounded-vee Wall Shapes, Numer. Heat Transfer A, vol. 63, no. 8, pp. 563–589, 2013.
[4]. L. Zhang and D. Che, Influence of Corrugation Profile on the Thermalhydraulic Performance of Cross-Corrugated Plates, Numer. Heat Transfer A, vol. 59, no. 4, pp. 267–296, 2011.
[5]. L. Zhang and D. Che, Turbulence Models for Fluid Flow and Heat Transfer between Cross-Corrugated Plates, Numer. Heat Transfer A, vol. 60, no. 5, pp. 410–440, 2011.
[6]. L. Chen, H. Luan, Y. L. He, and W. Q. Tao, Effects of Roughness of Gas Diffusion LayerSurface on Liquid Water Transport in Micro Gas Channels of a Proton Exchange MembraneFuel Cell, Numer. Heat Transfer A, vol. 62, no. 4, pp. 295–318, 2012.
[7]. M. B. Turgay and A. G. Yazicioglu, Effect of Surface Roughness in Parallel-Plate Micro-channelson Heat Transfer, Numer. Heat Transfer A, vol. 56, no. 6, pp. 497–514, 2009.
[8]. A. Keshmiri and J. Gotts, Thermalhydraulic Analysis of Four Geometrical Design Parameters in Rib-Roughened Channels, Numer. Heat Transfer A, vol. 60, no. 4, pp.305–327, 2011.
[9]. V. S. Hans, R. P. Saini, and J. S. Saini, Performance of Artificially Roughened Solar Air Heaters—A Review, Renewable and Sustainable Energy Reviews, vol. 13, pp. 1854–1869, 2009.
[10]. B. Bhushan and R. Singh, A Review on Methodology of Artificial Roughness used in Duct of Solar Air Heaters, Energy, vol. 35, pp. 202–212, 2010.
[11]. A. Kumar, R. P. Saini, and J. S. Saini, Heat and Fluid Flow Characteristics of RoughenedSolar Air Heater Ducts—A review, Renewable Energy, vol. 47, pp. 77–94, 2012.
[12]. A. S. Yadav and J. L. Bhagoria, A CFD Analysis of a Solar Air Heater having TriangularRib Roughness on the Absorber Plate, Int. J. of Chem Tech Research, vol. 5, no. 2,pp. 964–971, 2013.
[13]. A. Chaube, P. K. Sahoo, and S. C. Solanki, Analysis of Heat Transfer Augmentation, andFlow Characteristics due to Rib Roughness over Absorber Plate of a Solar Air Heater, Renewable Energy, vol. 31, pp. 317–331, 2006.
[14]. A. S. Yadav, and J. L. Bhagoria, A CFD-Based Heat Transfer, and Fluid Flow Analysisof a Solar Air Heater Provided with Circular Transverse Wire Rib Roughness on the
[15]. Absorber Plate, Energy, vol. 55, pp. 1127–1142, 2013.
[16]. S. Kumar, and R. P. Saini, CFD-Based Performance Analysis of a Solar Air Heater Duct provided with Artificial Roughness, Renewable Energy, vol. 34, pp. 1285–1291, 2009.
[17]. A. S. Yadav, and J. L. Bhagoria, A CFD-Based Heat Transfer, and Fluid Flow Analysis of a Conventional Solar Air Heater, J. of Eng. Sci. and Management Education, vol. 6, no. 2, pp. 138–147, 2013.
[18]. S. V. Karmare and A. N. Tikekar, Analysis of Fluid Flow and Heat Transfer in a Rib GritRoughened Surface Solar Air Heater using CFD, Solar Energy, vol. 84, pp. 409–417, 2010.
[19]. A. S. Yadav and J. L. Bhagoria, Numerical Investigation of Flow through an Artificially Roughened Solar Air Heater, Int. J. of Ambient Energy, in press (doi:10.1080=01430750.2013.823107).
[20]. B. K. Gandhi and K. M. Singh, Experimental and Numerical Investigations on Flowthrough Wedge Shape Rib Roughened Duct, The Institution of Engineers (India)J. MC, vol. 90, pp. 13–18, 2010.
[21]. A. S. Yadav and J. L. Bhagoria, Heat Transfer and Fluid Flow Analysis of Solar Air Heater: A Review of CFD Approach, Renewable and Sustainable Energy Reviews,vol. 23, pp. 60–79, 2013.
[22]. ASHRAE Standard 93, Method of Testing to Determine the Thermal Performance of Solar Collectors, American Society of Heating, Refrigeration and Air Conditioning Engineers, Atlanta, GA30329, 2003.
[23]. D. Gupta, S. C. Solanki, and J. S. Saini, Thermohydraulic Performance of Solar Air Heaters with Roughened Absorber Plates, Solar Energy, vol. 61, no. 1, pp. 33–42, 1997.
[24]. ANSYS FLUENT 2022, Documentation, ANSYS, Inc. 2022–04.
[25]. B. E. Launder, and D. B. Spalding, Lectures in Mathematical Models of Turbulence, Academic Press, London, 1972.
[26]. S. V. Patankar, Numerical Heat Transfer and Fluid Flow, Hemisphere, Washington, D.C.1980.
[27]. R. L. Webb and E. R. G. Eckert, Application of Rough Surface to Heat Exchanger Design, Int. J. of Heat and Mass Transfer, vol. 15, pp. 1647–1658, 1972.
[28]. W. H. McAdams, Heat Transmission, McGraw-Hill, New York, 1942.
[29]. W. Fox, P. Pritchard, and A. McDonald, Introduction to Fluid Mechanics, pp. 754, John Wiley & Sons, New York, 2010.
[30]. M. J. Nine, G. H. Lee, H. S. Chung, M. Ji, and H. Jeong, Turbulence and Pressure Drop Behaviors around Semicircular Ribs in a Rectangular Channel, Thermal Science, in press (doi:10.2298=TSCI111022142N).
[31]. S. W. Ahn, The Effects of Roughness Types on Friction Factors and Heat Transfer in Roughened Rectangular Duct, Int. Comm. in Heat and Mass Transfer, vol. 28, no. 7, pp. 933–942, 2001.